ADVANCED FUNCTIONAL MATERIALS

FULL PAPER

DOI: 10.1002/adfm.200701137

Electrophosphorescent Polyfluorenes Containing Osmium Complexes in the Conjugated Backbone**

By *Chen-Han Chien, Song-Fu Liao, Chen-Hao Wu, Ching-Fong Shu,* Sheng-Yuan Chang, Yun Chi,* Pi-Tai Chou,** and *Cheng-Hsuan Lai*

Electrophosphorescent copolymers have been synthesized by covalent bonding of a red-emitting osmium complex Os(bpftz), which contains two 3-trifluoromethyl-5-(4-*tert*-butyl-2-pyridyl)triazolate (bpftz) cyclometalated ligands, into the backbone of a bipolar polyfluorene (PF) copolymer. Employing these copolymers, a highly efficient red polymer light-emitting diode has been realised that has an external quantum efficiency of 18.0%, a maximum brightness of 38 000 cd m^{-2}, and an emission centered at 618 nm. In addition, after incorporating appropriate amounts of green-emitting benzothiadiazole (BT) and the aforementioned Os(bpftz) into the bipolar PF, an efficient white-light electroluminescent polymer is obtained that displays simultaneous blue, green, and red emissions.

1. Introduction

Recently, electrophosphorescent organic light-emitting diodes (OLEDs) that utilize heavy metal phosphors as their light-emitting components have become a topical subject because of their high quantum efficiencies.[1–3] The strong spin-orbit coupling induced by heavy metal ions, such as iridium(III), promotes an increase in the efficient intersystem crossing from the singlet to the triplet excited state, which then facilitates strong electroluminescence by harnessing both the singlet and triplet excitons after initial charge recombination. These heavy metal-containing emitters are considered to be superior to their fluorescent counterparts for use in future OLED applications because, in theory, their internal phosphorescence quantum efficiencies (η_{int}) could reach as high as 100%.[4–6] As a result, there is a continuous trend of shifting OLED research toward studies of suitable heavy transition metal complexes.

Among the electrophosphorescent OLEDs, devices based on 'small molecules' have received the most attention to date, despite that this technology requires vacuum deposition of multilayer structures, a process that increases fabrication costs. On the other hand, devices based on semiconductor polymers (PLEDs) are of particular interest for their ready solution processability, which allows the utilization of less expensive spin-coating and ink-jet printing methods for the preparation of large-area devices.[7–10] Although polymeric diodes that feature phosphorescent dyes physically doped into the polymer hosts have been utilized to realize high efficiencies, such blend systems might suffer from aggregation of the phosphor and/or phase separation, which results in device instability. In efforts to overcome these shortcomings, new classes of polymeric electrophosphorescent materials with the phosphors covalently attached to the polymer backbone are being intensively investigated. Most of the polymers that have been developed are derived from polyfluorenes (PFs) that incorporate iridium-based complexes. PFs are often chosen as hosts because they exhibit large bandgaps, high photoluminescence (PL) and electroluminescence (EL) efficiencies, high thermal stabilities, as well as good solubility and film-forming properties.[11–14] Moreover, they are readily color-tuned through chemical incorporation of low bandgap co-monomers.[15–20] Electrophosphorescent PFs that feature cyclometalated iridium(III) complexes—either grafted on the side chain or incorporated into the conjugated backbone—have been thoroughly examined.[21–25] More recently, white-emitting PLEDs that employ a single polymer system containing a red-emitting iridium component have also been reported.[26–28]

Parallel to the studies that employ luminescent Ir^{III} complexes, we have been focusing on the design, preparation,

[*] Prof. C.-F. Shu, C.-H. Chien, S.-F. Liao, Chen-Hao Wu
Department of Applied Chemistry
National Chiao Tung University
Hsinchu, 300 (Taiwan ROC)
E-mail: shu@cc.nctu.edu.tw
Prof. Y. Chi, S.-Y. Chang
Department of Chemistry
National Tsing Hua University
Hsinchu, 300 (Taiwan ROC)
E-mail: ychi@mx.nthu.edu.tw
Prof. P.-T. Chou, C.-H. Lai
Department of Chemistry
National Taiwan University
Taipei, 106 (Taiwan ROC)
E-mail: chop@ntu.edu.tw

[**] The authors thank the National Science Council for financial support. Special thanks go to Professor C.-H. Cheng for his support and assistance during the preparation and characterization of the light-emitting devices.

ADVANCED FUNCTIONAL MATERIALS

and evaluation of less-accessible Os^{II} emitting materials.[29–35] Because of its divalent state, the oxidation potential at the Os^{II} metal center is significantly lower compared with that of the trivalent Ir^{III} analogues. This property might reduce the radiative lifetime of Os^{II} complexes relative to that of the corresponding Ir^{III} systems, because of the enhanced degree of the heavy metal atom's participation in the lowest excited triplet manifolds.[35] The shortened radiative lifetime should reduce the extent of triplet–triplet annihilation for devices that have a higher dopant concentration or under a higher current density. In addition, the cathodic-shifted oxidation potential increases the energy level of the HOMO, making it suitable for neutral Os^{II} complexes to serve as sites for direct charge trapping. Consequently, highly emissive Os^{II} complexes are among the best emitting dopants for phosphorescent OLEDs.[33,34,36]

In this paper, we report the preparation of electrophosphorescent copolymers TOF-Os(bpftz)$_x$ through covalent incorporation of a red-emitting osmium complex (Os(bpftz), at concentrations of 1.0–2.0 mol%) into the backbone of a blue-emitting PF copolymer (PF-TPA-OXD) that presents both hole- and electron-transporting pendent groups. Using these copolymers, a highly efficient red-emitting PLED is realized that exhibits an external quantum efficiency of 18.0% and Commission Internationale d'Énclairage (CIE) coordinates of (0.64, 0.35). In addition, we also observed efficient white-light electrophosphorescence from a TOF-Os(bpftz)$_x$ copolymer that contains an additional green-emitting benzothiadiazole (BT) moiety covalently bonded to the bipolar PF polymer.

2. Results and Discussion

2.1. Synthesis of the Os-Containing Copolymers

The synthesis of the Os^{II} complex M1 was initiated through reaction of $Os_3(CO)_{12}$ with 3-trifluoromethyl-5-(4-*tert*-butylpyridyl)-1,2,4-triazole (bpftz)[35] to form the complex $Os(bpftz)_2(CO)_2$. Subsequent treatment with freshly sublimed Me_3NO to eliminate the CO ligands, followed by addition of (4-bromophenyl)diethylphosphine at the diaxial positions, gave the required M1. The triphenylamine (TPA)-containing M2,[37] the oxadiazole (OXD)-containing M3,[38] and the diboronate M4[39] were synthesized according to reported procedures. Scheme 1 illustrates the synthetic route for the

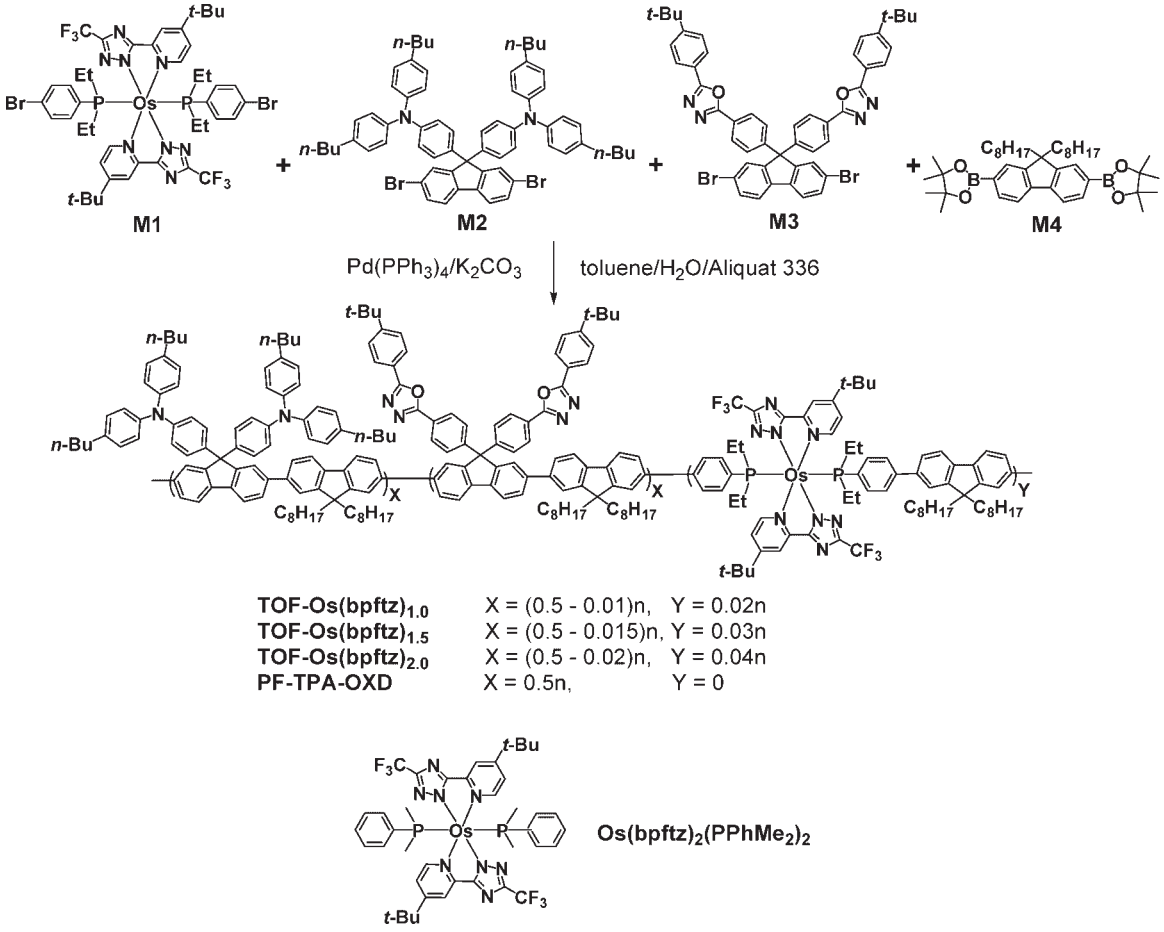

Scheme 1. Synthetic route of Os-attached copolymers and chemical structure of the model compound.

TOF-Os(bpftz)$_x$ copolymers, and includes the feed ratios of all co-monomers. The copolymers TOF-Os(bpftz)$_x$ that incorporate red-emitting Os moieties in the PF backbone were synthesized by Suzuki coupling polymerization between the dibromides M1 and M3 and the diboronate M4. These copolymerizations were undertaken using $Pd(PPh_3)_4$ as the catalyst and Aliquat 336 as the phase-transfer reagent in a mixture of toluene and 2.0 M aqueous K_2CO_3. The resultant random copolymers possess backbones that consist of fluorene segments of various lengths separated by a chelating Os complex at both ends of each segment. The osmium contents in the copolymers (0.35–0.62 wt%, measured using inductively coupled plasma mass spectrometry (ICP-MS)), matched the applied monomer feed ratios (0.32–0.64 wt%). For the sake of comparison, we also prepared the blue-light-emitting polymer PF-TPA-OXD through copolymerization of the monomers M2, M3, and M4, as reported previously.[37]

The TOF-Os(bpftz)$_x$ copolymers readily dissolved in common organic solvents, such as tetrahydrofuran (THF), chloroform, toluene, and chlorobenzene. Their number-average molecular weights (M_n), determined using size exclusion chromatography (SEC, eluent: THF) and calibrated against polystyrene standards, were in the range (4.1–5.8) $\times$ 10^4 g mol^{-1}, with polydispersities that ranged from 1.38 to 1.67 (Table 1). As revealed by thermogravimetric analysis (TGA), the polymers exhibited good thermal properties, with 5% weight losses at temperatures above 410 °C. The glass transition temperatures (T_gs) of the TOF-Os(bpftz)$_x$ systems, determined using differential scanning calorimetry (DSC), were ~180 °C (Table 1), i.e., close to that of PF-TPA-OXD.[37] This result indicates that the incorporation of such a small amount of the Os complex does not alter the rigidity of the resulting copolymers. Moreover, such a high-temperature glass transition temperature can prevent morphological changes upon exposure to excessive heat treatment, which is desirable for polymers used in light-emitting applications.

2.2. Optical Properties

Figure 1a depicts the absorption and emission spectra of TOF-Os(bpftz)$_x$ in CH_2Cl_2, while pertinent spectroscopic and dynamic data are summarized in Table 2. The Os-containing copolymers exhibit absorption spectroscopic features that are similar to those observed for PF-TPA-OXD, which consist of two major absorption bands at ~305 and 390 nm, which originate from the absorptions of the charge-transporting pendent groups (TPA and OXD) and the conjugated PF backbone, respectively.[37] The absorption of the Os(bpftz) moiety is barely observable because of its low concentration in the copolymers. The Os(bpftz)-containing copolymers in degassed CH_2Cl_2 solution exhibit a notable blue emission and a weak red emission with peak wavelengths around 450 and 620 nm, respectively. Figure 1b shows the PL spectra of TOF-Os(bpftz)$_x$ versus that of PF-TPA-OXD in the solid film. The corresponding photophysical data are summarized in Table 2.

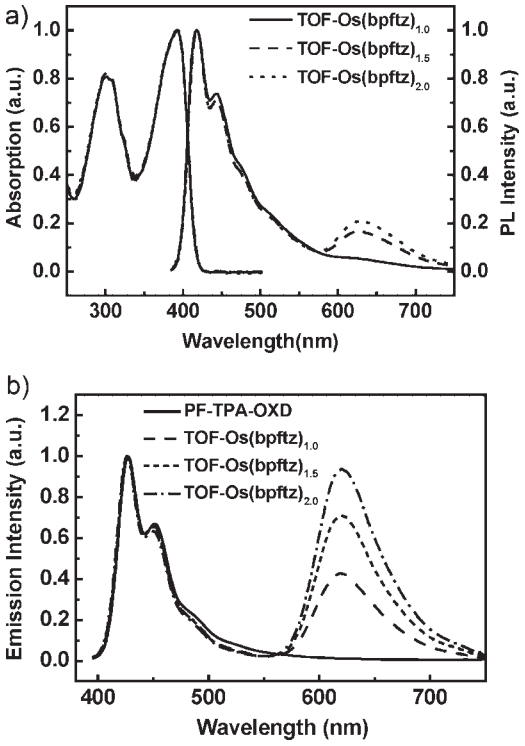

Figure 1. a) Absorption and emission spectra of TOF-Os(bpftz)$_x$ copolymers in degassed CH_2Cl_2. b) Solid-state PL spectra of TOF-Os(bpftz)$_x$ copolymers and PF-TPA-OXD (excited at 380 nm).

Table 1. Molecular weight and thermal properties of Os-attached copolymers.

Polymer	M_w[a]	M_n[a]	M_w/M_n[a]	T_g[b] (DSC)	$T_{d,5\%}$[c] (TGA)
TOF-Os(bpftz)$_{1.0}$	80 000	58 000	1.38	182	419
TOF-Os(bpftz)$_{1.5}$	78 000	54 000	1.46	179	404
TOF-Os(bpftz)$_{2.0}$	68 000	45 000	1.51	178	404
TOF-W	68 000	41 000	1.67	190	439

[a]The molecular weight (g mol^{-1}) was determined by SEC in THF. [b]T_g (°C) was determined by DSC at a heating rate of 10 °C min^{-1} under nitrogen. [c]Temperature at which a 5% weight loss was detected at a heating rate of 10 °C min^{-1} under nitrogen.

The PL spectra of TOF-Os(bpftz)$_x$ films contain a strong emission band centered at 620 nm as a result of the triplet emission of Os(bpftz), in addition to the blue emission (two vibronic peaks at 427 and 450 nm). In contrast to the major blue band in CH_2Cl_2, the intensity of the blue and red emission is of the same magnitude. For comparison, PF-TPA-OXD, which is considered to have emission solely from the PF backbone, exhibits blue emission that is identical to that of TOF-Os(bpftz)$_x$ (427 and 450 nm). Moreover, as shown in Figures 1a and 1b, the intensity of the red emission increases as the content of the Os complex increases. Accordingly, the blue and red emission bands originate from the conjugated PF backbone and Os(bpftz) moiety, respectively. The excitation

ADVANCED FUNCTIONAL MATERIALS

Table 2. Photophysical behaviors of Os-attached copolymers.

Polymer	Solution[a]				Film[b]			
	λ_{abs} [nm]	λ_{em} [nm]	Φ_F	τ_{obs} [ns]	λ_{abs} [nm]	λ_{em} [nm]	Φ_F	τ_{obs} [ns]
TOF-Os(bpftz)$_{1.0}$	300, 391	417, 442	0.72	τ_{450}: 9 τ_{650}: 656	305, 391	427, 450, 618	0.19	τ_{450}: 0.14 τ_{650}: 489
TOF-Os(bpftz)$_{1.5}$	300, 391	416, 441, 623	0.74	τ_{450}: 9 τ_{650}: 780	305, 391	427, 451, 618	0.17	τ_{450}: 0.3 τ_{650}: 527
TOF-Os(bpftz)$_{2.0}$	300, 391	417, 442, 623	0.75	τ_{450}: 10 τ_{650}: 789	305, 391	427, 452, 618	0.21	τ_{450}: 0.27 τ_{650}: 541
TOF-W	301, 391	416, 443	0.79	τ_{450}: 8.5 τ_{650}: 750	303,391	427, 451, 519, 607	0.39	τ_{450}: 0.14 τ_{650}: 490

[a]Data obtained in degassed CH_2Cl_2 at ambient temperature. [b]Evaluated in the solid state using films prepared through spin-coating from toluene solutions.

spectra of TOF-Os(bpftz)$_x$ monitored at either 450 or 620 nm emission, within experimental error, are also effectively identical to the absorption spectrum (not shown here). The results, in a qualitative manner, support an efficient energy transfer between the polymer backbone and Os complex. To understand the interactions between Os(bpftz) and PF, we prepared a model compound, Os(bpftz)$_2$(PPhMe$_2$)$_2$, to investigate the optical behavior of the red-emitting moieties in the dye-incorporated copolymers. Figure 2 displays the optical properties of Os(bpftz)$_2$(PPhMe$_2$)$_2$ in dilute CH_2Cl_2 solution and the emission spectrum of PF-TPA-OXD in the solid state. The absorption spectrum of Os(bpftz)$_2$(PPhMe$_2$)$_2$ overlaps well with the emission spectrum of PF-TPA-OXD at 400–500 nm. This finding further implies that energy transfer may occur from the excited singlet state of the PF polymer to the excited singlet state of the Os complex, followed by fast intersystem crossing and, consequently, emission from its triplet excited state. We note that there is negligible red shift for the signal of the Os complex in the doped copolymers relative to that of the model Os complex, presumably because the lower lying triplet metal-to-ligand charge transfer (^{3}MLCT) inherently possesses electronic transition from osmium metal to the π^* orbital of the pyridyl group of bpftz ligand; the latter shows no extended conjugation to the PF backbone.[35] Moreover, the auxiliary phosphines serve as insulators and do not cause any additional shifting of emission wavelength.

2.3. Electroluminescence Properties

PLEDs that have the configuration indium tin oxide (ITO)/poly(styrene-sulfonate)-doped poly(3,4-ethylenedioxythiophene) (PEDOT:PSS, 35 nm)/TOF-Os (bpftz)$_x$ (50–70 nm)/1,3,5-tris(1-phenyl-1H-benzimidazol-2-yl) benzene (TPBI, 30 nm)/LiF (15 Å)/ Al (100 nm) were fabricated to investigate the EL performance of the copolymers. Figure 3 depicts the corresponding EL spectra recorded at 9 V. In the case of TOF-Os(bpftz)$_{1.0}$, the EL spectra exhibit emissions that arise mainly from the Os dopant at 618 nm, together with a very minor contribution from the PF backbone. The host EL emission was quenched completely at an Os(bpftz) content of 1.5 mol%. The dramatic difference between the EL and PL spectra of the copolymers reveals that the dominant mechanism involved in the electroluminescence process was direct charge-trapping/recombination at the Os(bpftz) sites,[36,40–42] rather than the Förster energy transfer from the fluorene segments to the low-bandgap triplet dopants, which occurred

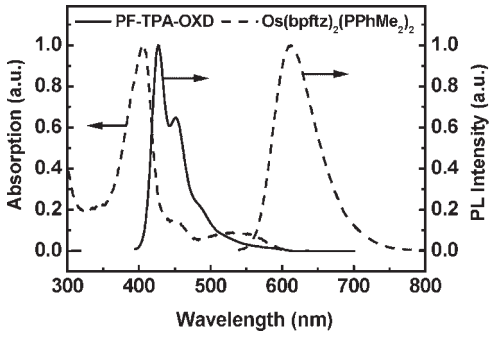

Figure 2. Absorption and PL spectra of the model compound Os(bpftz)$_2$(PPhMe$_2$)$_2$ in CH_2Cl_2 solution and the solid-state emission spectrum of PF-TPA-OXD.

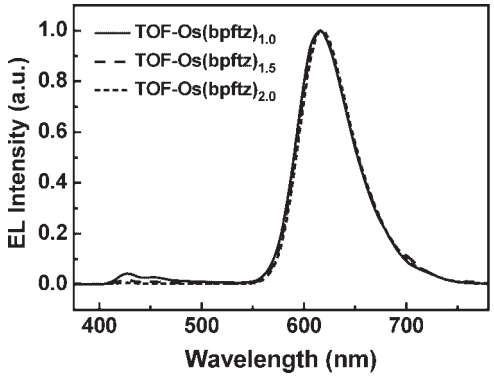

Figure 3. EL spectra of ITO/PEDOT/TOF-Os(bpftz)$_x$/TPBI/LiF/Al devices recorded at an applied potential of 9 V.

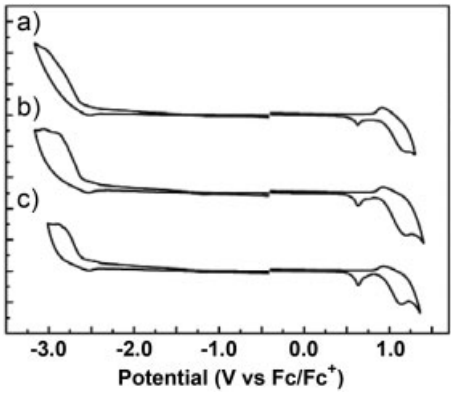

Figure 4. Cyclic voltammograms of a) TOF-Os(bpftz)$_{1.0}$, b) TOF-Os(bpftz)$_{1.5}$, and c) TOF-Os(bpftz)$_{2.0}$ films coated on a glassy carbon electrode.

under photoexcitation. To further understand the details of the EL mechanism, we employed cyclic voltammetry (CV) to measure the HOMO and LUMO energy levels of TOF-Os(bpftz)$_x$. The electrochemical processes of this polymer film coated on a glassy carbon electrode were monitored in a standard three-electrode electrochemical cell using ferrocene as the internal standard. TOF-Os(bpftz)$_x$ exhibited almost the same redox behavior as PF-TPA-OXD,[37] with onset potentials for oxidation and reduction of 0.50 and –2.33 eV, respectively (Fig. 4). Based on these values, we estimated the HOMO and LUMO energy levels of the three copolymers to be approx. −5.30 and −2.47 eV, respectively, in relation to the energy level of the ferrocene reference (4.80 eV below the vacuum level).[43] The HOMO level reflects the electron-rich nature of the TPA moiety, while the LUMO level reflects the electron-deficient nature of the pendent OXD units.[37] We did not observe any electrochemical behavior attributable to the Os dopant in TOF-Os(bpftz)$_x$, possibly because of its low content in the polymer backbones. Instead, we utilized the HOMO and LUMO levels of the model compound Os(bpftz)$_2$(PPhMe$_2$)$_2$ — deduced from CV measurements to be –4.84 and –2.10 eV, respectively — as the energy levels of the Os complexes embedded in the PF backbone. Figure 5 illustrates the energy level diagram of the materials involved in

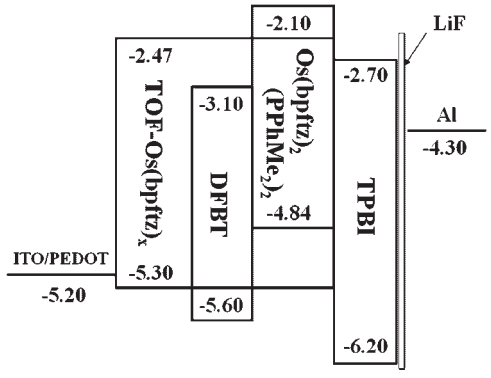

Figure 5. Energy level diagram for the materials involved in EL devices.

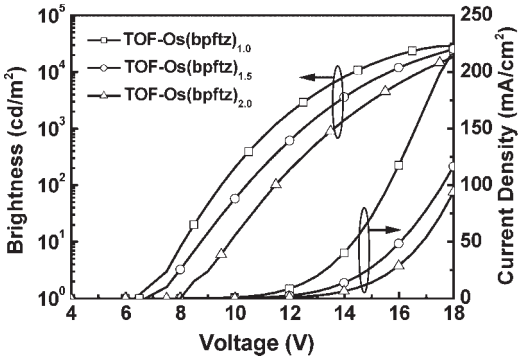

Figure 6. Current density–voltage–luminance characteristics of the PLEDs based on TOF-Os(bpftz)$_x$ copolymers.

the EL devices, which indicates that the Os-containing phosphor may function as a hole trap in the PF-TPA-OXD host. For devices that have the configuration ITO/PEDOT/TOF-Os(bpftz)$_x$/TPBI/LiF/Al, holes are readily injected from PEDOT (−5.20 eV)[44] into the HOMOs of the TPA moieties (−5.30 eV) of PF-TPA-OXD upon overcoming a small energy barrier (0.10 eV). Because the ionization potential of the Os(bpftz) complex (−4.84 eV) is 0.46 eV above the HOMO of PF-TPA-OXD, the holes might subsequently become trapped at the Os(bpftz) unit, followed by recombination of opposite charges (electrons) to form excitons.[36]

Figure 6 presents the current density–voltage–luminance (*I–V–L*) characteristics of the TOF-Os(bpftz)$_x$-based electrophosphorescent devices. The features in the current density vs. voltage (*I–V*) plot shifted to higher voltages upon increasing the doping concentration of Os(bpftz) in the polymer host. This result is consistent with the charge trapping mechanism proposed previously from the dramatic difference between the observed PL and EL spectra.[36,40–42] Table 3 summarizes the performances of the electrophosphorescent devices based on TOF-Os(bpftz)$_x$. Figure 7 presents plots of the external quantum efficiency (η_{ext}) and luminance efficiency as functions of the current density. The best device performance was achieved using TOF-Os(bpftz)$_{1.5}$, which showed a turn-on voltage of 7.1 V (which corresponds to 1 cd m^{-2}) and a red emission that is characteristic of the Os(bpftz) unit exclusively, while reaching a maximum brightness of 38 084 cd m^{-2} at 20 V. At a current density of 9.3 mA cm^{-2}, we obtained a maximum value of η_{ext} of 18.0% (which corresponds to a luminance efficiency of 26.3 cd A^{-1}), together with a brightness of 2447 cd m^{-2}. Even at a much higher current density of 100 mA cm^{-2}, more than 80% of the peak efficiency (14.9%) was sustained, with a bright phosphorescence of ~22 000 cd m^{-2}. Thus, the TOF-Os(bpftz)$_{1.5}$-based device exhibited significantly improved efficiency and brightness relative to those of the electrophosphorescent devices derived from polymers that possess iridium metal complexes.[21–25] We attribute this superior performance to the presence of the highly efficient Os phosphor, and its shorter triplet lifetime helped to minimize the degree of exciton quenching through triplet–triplet annihilation at a high current density.[45,46] In addition, the

Table 3. Performance of TOF-Os(bpftz)$_x$-based devices that have the structure ITO/PEDOT/polymer/TPBI/LiF/Al.

Parameter	Red			White
	TOF-Os(bpftz)$_{1.0}$	TOF-Os(bpftz)$_{1.5}$	TOF-Os(bpftz)$_{2.0}$	TOF-W
Turn-on voltage [V][a]	6.5	7.1	7.5	5.6
Voltage [V][b]	13.0 (15.6)	14.5 (17.6)	15.5 (18.1)	9.4 (11.8)
Brightness [cd m^{-2}][b]	4317 (17841)	5180 (22281)	4433 (19384)	2008 (8094)
L. E. [cd A^{-1}][b]	21.6 (17.9)	25.9 (22.3)	22.2 (19.4)	10.0 (8.1)
E. Q. E. [%][b]	14.0 (11.6)	17.4 (14.9)	15.2 (13.3)	5.1 (4.1)
Max. brightness [cd m^{-2}]	29 075 (18 V)	38 084 (20 V)	34 437 (20 V)	8447 (12.5 V)
Max. L. E. [cd A^{-1}]	22.6	26.3	22.6	10.7
Max. E. Q. E. [%]	14.6	18.0	15.4	5.4
EL maximum [nm][c]	430, 618	618	618	428, 454, 518, 614
CIE, x and y[c]	(0.62, 0.34)	(0.64, 0.35)	(0.65, 0.35)	(0.37, 0.30)

[a]Recorded at 1 cd m^{-2}. [b]Recorded at 20 mA cm^{-2}; data in parentheses were recorded at 100 mA cm^{-2}. [c]Recorded at 9 V.

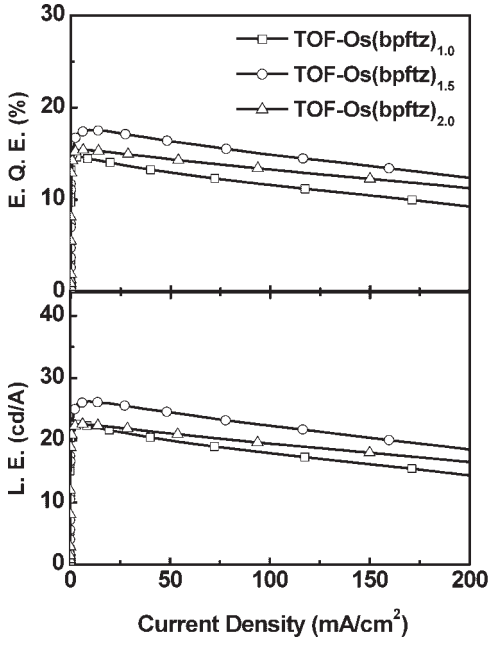

Figure 7. External quantum efficiency and luminance efficiency plotted as functions of the current density for the PLEDs based on TOF-Os(bpftz)$_x$.

bipolar polymeric host facilitated charge injection in the emitting layer. The presence of the hole/exciton-blocking (TPBI) layer also effectively confines the excitons within the emitting layer.

2.4. White Electroluminescent PF Copolymer

We next realized an efficient white-light-emitting polymer (TOF-W) obtained by covalently attaching appropriate amounts of both a green fluorophore, BT, and our red phosphor, Os(bpftz) (concentrations of 0.01 and 0.02 mol%, respectively), into the backbone of the blue-emitting PF-TPA-OXD polyfluorene. This custom-made copolymer was prepared using monomers M1–M5 through Suzuki polycondensation (Scheme 2). As depicted in Figure 8, the TOF-W-based device that had the configuration ITO/PEDOT (35 nm)/TOF-W (50–70 nm)/TPBI (30 nm)/LiF (15 Å)/Al (100 nm) exhibited broadened emissions covering the region 400–700 nm with main peaks — centered at 428, 518, and 614 nm — lying within the ranges of the three primary colors. We assign the peak in the blue region to the characteristic emission of the PF moieties and the other two peaks in the green and red regions to the BT and Os(bpftz) units, respectively. Compared with the PL spectra

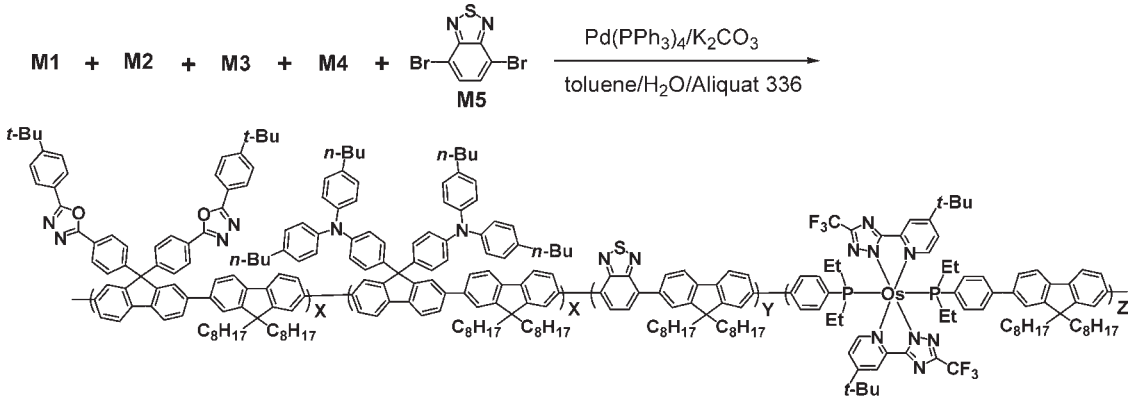

Scheme 2. Synthetic route of the white-light-emitting polyfluorene copolymers.

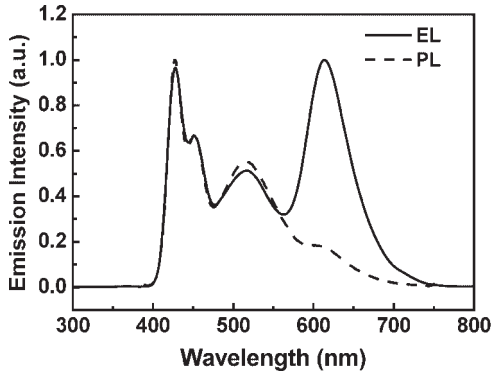

Figure 8. EL and PL spectra of the TOF-W film.

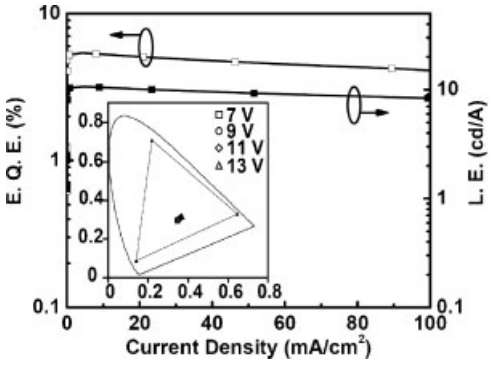

Figure 10. Luminance efficiency and external quantum efficiency plotted as a function of the current density for the white-light-emitting device. Inset: variation in CIE color coordinates of the TOF-W device as the bias increased from 7 to 13 V.

in the solid state, the contribution from the red-emitting Os(bpftz) was dramatically enhanced in the EL spectra. As demonstrated above, instead of Förster energy transfer, direct charge-trapping/recombination at the Os(bpftz) moieties was the dominant mechanism responsible for the red electrophosphorescence. On the other hand, the green emission was not preferentially populated in the EL spectrum when compared with the PL spectrum. We utilized the HOMO and LUMO energy levels of the green-emitting model compound 4,7-bis (9,9-dihexylfluoren-2-yl)-2,1,3-benzothiadiazole (DFBT)—reported previously to be −5.60 and −3.10 eV, respectively—as the energy levels of the BT units embedded in the PF backbone.[28,47] According to the energy diagram displayed in Figure 5, it is not possible for the BT-based units to play any role in trapping the hole carrier. This finding is consistent with our previous observation of only slight differences between the EL and PL spectra of the individual polymers,[47] which suggests that Förster energy transfer was the main operating process for generation of the green electroluminescence.

The EL spectrum of the TOF-W-based device displayed an emission envelope that covered the whole visible region. The CIE chromaticity of (0.37, 0.30) at a bias of 9 V fell in the white light region. Figure 9 displays the *I–V–L* curves of the white-light-emitting device, which reveals a turn-on voltage of 5.6 V (corresponding to 1 cd m^{-2}) and a brightness of 1000 cd m^{-2} achieved at ~8.6 V. Table 3 summarizes the key characteristics of the white-light-emitting device. Moreover, as plotted in Figure 10, the maximum luminance efficiency of 10.7 cd A^{-1}, which corresponds to an external quantum efficiency of 5.4%, was obtained from the TOF-W device at a bias of 8 V, a current density of 4.1 mA cm^{-2}, and a brightness of 442 cd m^{-2}. The EL efficiency of the TOF-W device is one of the highest values reported for a white electroluminescent device based on a single-component polymer, for which their constituents are provided by the three primary colors.[18,26–28,47–49] Finally, at a much higher current density of 100 mA cm^{-2}, more than 80% of the peak efficiency (8.1 cd A^{-1}) was sustained, with a brightness of ~8094 cd m^{-2}. 2. The inset of Figure 10 indicates the minor shift of the CIE coordinates from (0.36, 0.29) at a voltage of 7.0 V (0.4 mA cm^{-2}, 32 cd m^{-2}) to (0.39, 0.32) upon increasing the driving voltage to 13 V (93.1 mA cm^{-2}, 8314 cd m^{-2}); nevertheless, the color coordinates remain in the white-light region.

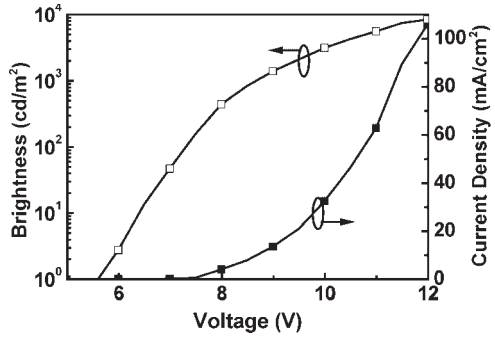

Figure 9. Current density–voltage–luminance characteristics of the PLED based on TOF-W.

3. Conclusions

Unlike the extensively investigated polymers that incorporate luminescent Ir^{III} complexes,[21–28] electrophosphorescent polymers based on Os^{II} emitting materials are much less developed and accessible—even though Os^{II} complexes exhibit desirably shorter triplet emission lifetimes and lower oxidation potentials.[29–35] In this study, we synthesized highly efficient electrophosphorescent PF derivatives TOF-Os(bpftz)$_x$ in which a red-emitting Os(bpftz) unit (at concentrations of 1.0–2.0 mol%) was covalently incorporated into the PF copolymer that contained both hole- and electron-transporting pendent groups. PLEDs that have the configuration ITO/PEDOT/TOF-Os(bpftz)$_x$/TPBI/LiF/Al were successfully fabricated. The optimized device with $x = 1.5$ exhibited the best performance: a maximum external quantum efficiency of 18.0% (which corresponds to a luminance efficiency of 26.3 cd A^{-1}), a

ADVANCED FUNCTIONAL MATERIALS

maximum brightness of 38 000 cd m^{-2}, and CIE chromaticity coordinates of (0.64, 0.35). Furthermore, through covalent attachment of a low concentration of a green-emitting BT unit and Os(bpftz) to the bipolar polyfluorene, we developed an efficient white-emitting polymer TOF-W which showed all blue, green, and red emissions. The maximum luminance efficiency was 10.7 cd A^{-1} (which corresponds to an external quantum efficiency of 5.4%) with a brightness of 442 cd m^{-2}, obtained at a current density of 4.1 mA cm^{-2}.

4. Experimental

Materials: 3-Trifluoromethyl-5-(4-*tert*-butylpyridyl)-1,2,4-triazole (bpftz), [35] the monomers M2, [37] M3, [38] M4, [39] and M5, [50] and the blue-light-emitting polymer PF-TPA-OXD [37] were prepared according to reported procedures. The solvents were dried using standard procedures. All other reagents were used as received from commercial sources, unless stated otherwise.

Characterization: ^{1}H, ^{13}C, ^{19}F, and ^{31}P NMR spectra were recorded on either a Varian Mercury 400 or INOVA 500 MHz spectrometer. Mass spectra were obtained using a JEOL JMS-HX 110 mass spectrometer. SEC was performed using a Waters chromatography unit interfaced to a Waters 410 differential refractometer; three 5 μm Waters styragel columns (300 × 7.8 mm^2) were connected in series in order of decreasing pore size (10^4, 10^3, and 10^2 Å), with THF as the eluent. Standard polystyrene samples were used for calibration. DSC was performed using a Seiko EXSTAR 6000 DSC unit operated at heating and cooling rates of 10 and 50 °C min^{-1}, respectively. Samples were scanned from 50 to 350 °C, cooled to 50 °C, and then scanned again from 50 to 350 °C. The T_gs were determined from the second heating scan. TGA was performed using a DuPont TGA 2950 instrument. The thermal stabilities of the samples under a nitrogen atmosphere were determined according to their weight losses while heating at a rate of 10 °C min^{-1}. UV-vis spectra were measured using a HP 8453 diode-array spectrophotometer. PL spectra were obtained using a Hitachi F-4500 luminescence spectrometer. Steady state absorption and emission spectra were recorded by a Hitachi (U-3310) spectrophotometer and an Edinburgh (FS920) fluorimeter, respectively. Both the wavelength-dependent excitation and emission responses of the fluorimeter were calibrated. An integrating sphere (Labsphere) was applied to measure the quantum yield excited by a 365 nm Ar^+ laser line. The resulting luminescence is acquired with a charge-coupled detector (Princeton Instruments, model CCD-1100) for subsequent quantum yield analyses. Lifetime studies were performed with an Edinburgh FL 900 photon-counting system with a hydrogen-filled or nitrogen lamp as the excitation source. CV measurements were performed using a BAS 100 B/W electrochemical analyzer operated at a scanning rate of 50 mV s^{-1}, employing 0.1 M tetrabutylammonium hexafluorophosphate ($TBAPF_6$) as the supporting electrolyte, and dissolved in anhydrous acetonitrile. The potentials were measured against an Ag/Ag^+ (0.01 M $AgNO_3$) reference electrode, with ferrocene as the internal standard. The onset potentials were determined from the intersection of two tangents drawn at the rising and background currents of the cyclic voltammogram.

Fabrication of PLEDs: PLEDs were fabricated in the structure ITO/poly(styrene sulfonate)-doped poly(3,4-ethylenedioxythiophene) (PEDOT:PSS; 35 nm)/polymer emitting layer (50–70 nm)/TPBI (30 nm)/LiF (15 Å)/Al (100 nm). The PEDOT was spin-coated directly onto indium tin oxide (ITO) glass and dried at 80 °C for 12 h under vacuum to improve both the hole injection capability and the smoothness of the substrate surface. The emissive layer was spin-coated on top of the PEDOT layer using chlorobenzene as the solvent. The sample was then dried for 3 h at 60 °C under vacuum. Prior to film casting, the polymer solution was filtered through a Teflon filter (0.45 μm). The TPBI, which was used as an electron-transporting layer that would also block holes and confine excitons, was grown through thermal sublimation in a vacuum of 3×10^{-6} torr. The cathode was completed through thermal deposition of LiF (15 Å)/Al (100 nm). The current–voltage–luminance relationships were measured under ambient conditions using a Keithley 2400 source meter and a Newport 1835C optical meter equipped with an 818ST silicon photodiode.

(4-Bromophenyl)diethylphosphine: *n*-BuLi (2.5 M in *n*-hexane, 3.2 mL, 8.00 mmol) was added dropwise at –78 °C under Ar to a stirred solution of 1,4-dibromobenzene (1.89 g, 8.00 mmol) in anhydrous THF (70 mL). The mixture was stirred at −78 °C for 1 h and then diethylphosphine chloride (1.00 g, 8.00 mmol) was added dropwise. The resulting mixture was gradually warmed to room temperature and stirring was continued for 12–16 h. The precipitated solid was filtered and then dried under vacuum to afford the title compound as an air-sensitive oily material (1.10 g, 56%). ^{1}H NMR (400 MHz, $CDCl_3$, δ): 7.44 (d, $J = 8.0$ Hz, 2H), 7.31 (dd, $J = 8.0$, 6.4 Hz, 2H), 1.63 (q, $J = 7.6$ Hz, 4H), 0.96 (dt, $J = 15.6$, 7.6 Hz, 6H). ^{31}P NMR (202 MHz, $CDCl_3$, δ): –16.20 (s).

Monomer M1: Pulverized $Os_3(CO)_{12}$ (100 mg, 0.11 mmol) was dissolved in anhydrous diethylene glycol monomethyl ether (DGME, 20 mL) and then added to a mixture of 3-trifluoromethyl-5-(4-*tert*-butylpyridyl)-1,2,4-triazole (bpftz, 191 mg, 0.71 mmol). The resulting solution was heated at 190–200 °C for 24 h under a nitrogen atmosphere. After cooling the mixture to room temperature, freshly sublimed Me_3NO (75.1 mg, 1.00 mmol) was added. The mixture was then heated at 100 °C for 2 h, followed by the addition of (4-bromophenyl)diethylphosphine (270 mg, 1.10 mmol). The solution was again heated at 190 °C for another 24 h. After cooling, the reaction mixture was dried under vacuum to provide a tarry product. Further purification by silica gel column chromatography (hexane/ethyl acetate, 4: 1), followed by recrystallization (hexane/ethyl acetate), afforded red-emitting crystals of M1 (230 mg, 57%). ^{1}H NMR (400 MHz, d_6-acetone, δ): 9.74 (d, $J = 6.0$ Hz, 2H), 7.72 (d, $J = 2.0$ Hz, Hz, 2H), 7.18 (dd, $J = 6.0$, 2.0 Hz, 2H), 7.10 (d, $J = 8.4$ Hz, 4H), 6.24–6.20 (m, 4H), 1.44 (s, 18H), 1.14–1.05 (m, 6H), 0.95–0.87 (m, 2H), 0.57–0.49 (m, 6H), 0.35–0.28 (m, 6H). ^{19}F NMR (470 MHz, d_6-acetone, δ): −63.35 (s, CF_3). ^{31}P NMR (202 MHz, d_6-acetone, δ): −8.60 (s). FAB MS (*m*/*z*): 1218 [M^+]. Anal. calcd. for $C_{44}H_{52}Br_2F_6N_8OsP_2$: C 43.36, N 9.19, H 4.30; found: C 43.95, N 9.32, H 4.49.

Model Compound Os(bpftz)$_2$(PPhMe$_2$)$_2$: A mixture of pulverized $Os_3(CO)_{12}$ (400 mg, 0.44 mmol) and 3-trifluoromethyl-5-(4-*tert*-butylpyridyl)-1,2,4-triazole (bpftz, 739 mg, 2.73 mmol) was dissolved in anhydrous diethylene glycol monomethyl ether (20 mL). The mixture was heated at 190–200 °C under nitrogen for 24 h. After cooling the reaction mixture to room temperature, freshly sublimed Me_3NO (199 mg, 2.65 mmol) was added. The solution was then heated at 100 °C for 1 h, followed by the addition of dimethylphenylphosphine (530 mg, 3.84 mmol). The resulting mixture was heated at 190 °C for 24 h. After cooling, the mixture was dried under vacuum to provide a tarry crude product. Further purification by silica gel column chromatography (hexane/ethyl acetate), followed by recrystallization (hexane/ethyl acetate, 4: 1), afforded red-emitting crystals of $Os(bpftz)_2(PPhMe_2)_2$ (800 mg, 60%). ^{1}H NMR (400 MHz, d_6-acetone, δ): 9.22 (d, $J = 6.0$ Hz, 2H), 7.60 (d, $J = 2.3$ Hz, 2H), 7.25 (dd, $J = 6.0$, 2.3 Hz, 2H), 7.07 (d, $J = 7.5$ Hz, 2H), 6.90 (d, $J = 7.5$ Hz, 4H), 6.35–6.31 (m, 4H), 1.39 (s, 18H), 0.87 (t, $J = 3.2$ Hz, 6H), 0.60 (t, $J = 3.2$ Hz, 6H). ^{19}F NMR (470 MHz, d_6-acetone, δ): −63.25 (s, CF_3). ^{31}P NMR (202 MHz, d_6-acetone, δ): −21.84 (s). FAB MS (*m*/*z*): 1006 [M^+], 868 [M^+ – $PPhMe_2$]. Anal. calcd. for $C_{40}H_{46}F_6N_8OsP_2$: C 47.80, N 11.15, H 4.61; found: C 47.50, N 10.87, H 5.00.

General Polymerization Procedure: Aqueous potassium carbonate (2.0 M, 1.80 mL) and Aliquat 336 (~20 mg) were added to a mixture of monomers M1–M5 in distilled toluene (5.6 mL). The mixture was degassed and then $Pd(PPh_3)_4$ (12 mg, 5.5 mol%) was added in one portion while flushing vigorously with nitrogen. The solution was heated at 75 °C for 24 h under nitrogen. The end groups were then capped by heating the mixture under reflux for 12 h with phenylboronic acid and then for 12 h with bromobenzene. The reaction mixture was

cooled to room temperature and the product was precipitated into a mixture of MeOH and H_2O [3: 7 (v/v), 100 mL]. The crude polymer was collected and washed with excess MeOH. The polymer was dissolved in THF, reprecipitated into MeOH, washed with acetone for 48 h using a Soxhlet apparatus, and then dried under vacuum to yield the desired copolymers.

TOF-Os(bpftz)$_{1.0}$: A mixture of monomers M1 (500 μL, 3.20 μmol, 6.40×10^{-3} M in toluene), M2 (79.1 mg, 76.4 μmol), M3 (67.0 mg, 76.4 μmol), and M4 (100 mg, 156 μmol) was copolymerized to yield TOF-Os(bpftz)$_{1.0}$ (179 mg, 96%). ^{1}H NMR (500 MHz, $CDCl_3$, δ): 0.71–0.78 (m, 20 H), 0.89–0.93 (m, 12 H), 1.07 (m, 40 H), 1.35 (m, 26 H), 1.56–1.59 (m, 8 H), 2.04 (m, 8 H), 2.53 (m, 8 H), 6.91–7.18 (m, 24H), 7.52–7.86 (m, 30H), 7.96–8.10 (m, 10H). ^{13}C NMR (125 MHz, $CDCl_3$, δ): 13.9, 14.0, 22.3, 22.5, 23.8, 29.1, 29.9, 31.0, 31.6, 31.7, 33.6, 35.0, 35.1, 40.2, 55.2, 55.3, 64.7, 65.8, 120.1, 121.4, 121.7, 122.9, 124.5, 124.6, 126.0, 126.2, 126.7, 127.2, 127.5, 128.8, 128.9, 129.0, 137.4, 138.4, 138.8, 140.2, 145.3, 146.7, 149.2, 150.7, 151.8, 152.8, 155.3, 164.0, 164.6. Anal. calcd: C 86.54, H 7.87, N 3.65; found: C 86.24, H 8.07, N 3.86.

TOF-Os(bpftz)$_{1.5}$: A mixture of monomers M1 (500 μL, 4.60 μmol, 9.20×10^{-3} M in toluene), M2 (78.4 mg, 75.7 μmol), M3 (66.4 mg, 75.7 μmol), and M4 (100 mg, 156 μmol) was copolymerized to yield TOF-Os(bpftz)$_{1.5}$ (166 mg, 89%). TOF-Os(bpftz)$_{1.5}$ exhibited ^{1}H and ^{13}C NMR spectra that were virtually identical to those of TOF-Os(bpftz)$_{1.0}$ because these two copolymers had very similar chemical structures and compositions.

TOF-Os(bpftz)$_{2.0}$: A mixture of monomers M1 (800 μL, 6.40 μmol, 8.0×10^{-2} M in toluene), M2 (77.4 mg, 74.8 μmol), M3 (65.6 mg, 74.8 μmol), and M4 (100 mg, 156 μmol) was copolymerized to yield TOF-Os(bpftz)$_{2.0}$ (171 mg, 92%). TOF-Os(bpftz)$_{2.0}$ exhibited ^{1}H and ^{13}C NMR spectra that were virtually identical to those of TOF-Os(bpftz)$_{1.0}$ because these two copolymers had very similar chemical structures and compositions.

TOF-W: A mixture of monomers M1 (670 μL, 0.67 μmol, 1.0×10^{-3} M in toluene), M2 (88.1 mg, 85.0 μmol), M3 (74.6 mg, 85.0 μmol), M4 (110 mg, 171 μmol), and M5 (330 μL, 0.33 μmol, 1.0×10^{-3} M in toluene) was copolymerized to yield TOF-W (190 mg, 94%). TOF-W exhibited ^{1}H and ^{13}C NMR spectra that were virtually identical to those of TOF-Os(bpftz)$_{1.0}$ because these two copolymers had very similar chemical structures and compositions.

Received: October 4, 2007
Revised: January 11, 2008

[1] M. A. Baldo, D. F. O'Brien, Y. You, A. Shoustikov, S. Sibley, M. E. Thompson, S. R. Forrest, *Nature* **1998**, *395*, 151.
[2] S. Lamansky, P. Djurovich, D. Murphy, F. Abdel-Razzaq, H.-E. Lee, C. Adachi, P. E. Burrows, S. R. Forrest, M. E. Thompson, *J. Am. Chem. Soc.* **2001**, *123*, 4304.
[3] E. Holder, B. M. W. Langeveld, U. S. Schubert, *Adv. Mater.* **2005**, *17*, 1109.
[4] N. J. Turro, *Modern Molecular Photochemistry*, University Science Books, Sausalito, CA **1991**.
[5] C. Adachi, M. A. Baldo, M. E. Thompson, S. R. Forrest, *J. Appl. Phys.* **2001**, *90*, 5048.
[6] Y. Kawamura, K. Goushi, J. Brooks, J. J. Brown, H. Sasabe, C. Adachi, *Appl. Phys. Lett.* **2005**, *86*, 071104.
[7] A. Kraft, A. C. Grimsdale, A. B. Holmes, *Angew. Chem. Int. Ed.* **1998**, *37*, 402.
[8] R. H. Friend, R. W. Gymer, A. B. Holmes, J. H. Burroughes, R. N. Marks, C. Taliani, D. D. C. Bradley, D. A. Dos Santos, J. L. Brédas, M. Lögdlund, W. R. Salaneck, *Nature* **1999**, *397*, 121.
[9] M. T. Bernius, M. Inbasekaran, J. O'Brien, W. Wu, *Adv. Mater.* **2000**, *12*, 1737.
[10] L. Akcelrud, *Prog. Polym. Sci.* **2003**, *28*, 875.
[11] Q. Pei, Y. Yang, *J. Am. Chem. Soc.* **1996**, *118*, 7416.
[12] D. Neher, *Macromol. Rapid Commun.* **2001**, *22*, 1365.
[13] M. Leclerc, *J. Polym. Sci, Part A: Polym. Chem.* **2001**, *39*, 2867.
[14] S. Becker, C. Ego, A. C. Grimsdale, E. J. W. List, D. Marsitzky, A. Pogantsch, S. Setayesh, G. Leizing, K. Müllen, *Synth. Met.* **2002**, *125*, 73.
[15] C. D. Müller, A. Falcou, N. Reckefuss, M. Rojahn, V. Wiederhirn, P. Rudati, H. Frohne, O. Nuyken, H. Becker, K. Meerholz, *Nature* **2003**, *421*, 829.
[16] C. Ego, D. Marsitzky, S. Becker, J. Zhang, A. C. Grimsdale, K. Müllen, J. D. MacKenzie, C. Silva, R. H. Friend, *J. Am. Chem. Soc.* **2003**, *125*, 437.
[17] R. Yang, R. Tian, J. Yan, Y. Zhang, J. Yang, Q. Hou, W. Yang, C. Zhang, Y. Cao, *Macromolecules* **2005**, *38*, 244.
[18] A. P. Kulkarni, X. Kong, S. A. Jenekhe, *Macromolecules* **2006**, *39*, 8699.
[19] M. C. Gather, A. Köhnen, A. Falcou, H. Becker, K. Meerholz, *Adv. Funct. Mater.* **2007**, *17*, 191.
[20] J. Liu, X. Guo, L. Bu, Z. Xie, Y. Cheng, Y. Geng, L. Wang, X. Jing, F. Wang, *Adv. Funct. Mater.* **2007**, *17*, **1917**.
[21] X. Chen, J.-L. Liao, Y. Liang, M. O. Ahmed, H.-E. Tseng, S.-A. Chen, *J. Am. Chem. Soc.* **2003**, *125*, 636.
[22] J. Jiang, C. Jiang, W. Yang, H. Zhen, F. Huang, Y. Cao, *Macromolecules* **2005**, *38*, 4072.
[23] H. Zhen, C. Jiang, W. Yang, J. Jiang, F. Huang, Y. Cao, *Chem. Eur. J.* **2005**, *11*, 5007.
[24] H. Zhen, C. Luo, W. Yang, W. Song, B. Du, J. Jiang, C. Jiang, Y. Zhang, Y. Cao, *Macromolecules* **2006**, *39*, 1693.
[25] G. L. Schulz, X. Chen, S.-A. Chen, S. Holdcroft, *Macromolecules* **2006**, *39*, 9157.
[26] J. Jiang, Y. Xu, W. Yang, R. Guan, Z. Liu, H. Zhen, Y. Cao, *Adv. Mater.* **2006**, *18*, 1769.
[27] H. Zhen, W. Xu, W. Yang, Q. Chen, Y. Xu, J. Jiang, J. Peng, Y. Cao, *Macromol. Rapid Commun.* **2006**, *27*, **2095**.
[28] F.-I. Wu, X.-H. Yang, D. Neher, R. Dodda, Y.-H. Tseng, C.-F. Shu, *Adv. Funct. Mater.* **2007**, *17*, 1085.
[29] S. Bernhard, X. Gao, G. G. Malliaras, H. D. Abruña, *Adv. Mater.* **2002**, *14*, 433.
[30] X. Jiang, A. K.-Y. Jen, B. Carlson, L. R. Dalton, *Appl. Phys. Lett.* **2002**, *80*, 713.
[31] B. Carlson, G. D. Phelan, W. Kaminsky, L. Dalton, X. Jiang, S. Liu, A. K.-Y. Jen, *J. Am. Chem. Soc.* **2002**, *124*, 14162.
[32] J. H. Kim, M. S. Liu, A. K.-Y. Jen, B. Carlson, L. R. Dalton, C.-F. Shu, R. Dodda, *Appl. Phys. Lett.* **2003**, *83*, 776.
[33] P.-T. Chou, Y. Chi, *Eur. J. Inorg. Chem.* **2006**, 3319.
[34] Y. Chi, P.-T. Chou, *Chem. Soc. Rev.* **2007**, *36*, 1421.
[35] P.-T. Chou, Y. Chi, *Chem. Eur. J.* **2007**, *13*, 380.
[36] F.-I. Wu, P.-I. Shih, Y.-H. Tseng, G.-Y. Chen, C.-H. Chien, C.-F. Shu, Y.-L. Tung, Y. Chi, A. K.-Y. Jen, *J. Phys. Chem. B* **2005**, *109*, 14000.
[37] C.-F. Shu, R. Dodda, F.-I. Wu, M. S. Liu, A. K.-Y. Jen, *Macromolecules* **2003**, *36*, 6698.
[38] F.-I. Wu, D. S. Reddy, C.-F. Shu, M. S. Liu, A. K.-Y. Jen, *Chem. Mater.* **2003**, *15*, 269.
[39] M. Ranger, D. Rondeau, M. Leclerc, *Macromolecules* **1997**, *30*, 7686.
[40] M. Uchida, C. Adachi, T. Koyama, Y. Taniguchi, *J. Appl. Phys.* **1999**, *86*, 1680.
[41] Y.-Y. Noh, C.-L. Lee, J.-J. Kim, K. Yase, *J. Chem. Phys.* **2003**, *118*, 2853.
[42] F.-C. Chen, S.-C. Chang, G. He, S. Pyo, Y. Yang, M. Kurotaki, J. Kido, *J. Polym. Sci, Part B: Polym. Phys.* **2003**, *41*, 2681.

ADVANCED FUNCTIONAL MATERIALS

[43] J. Pommerehne, H. Vestweber, W. Guss, R. F. Mahrt, H. Bässler, M. Porsch, J. Daub, *Adv. Mater.* **1995**, *7*, 551.
[44] M. T. Brown, J. S. Kim, R. H. Friend, F. Cacialli, R. Daik, W. J. Feast, *Appl. Phys. Lett.* **1999**, *75*, 1679.
[45] M. A. Baldo, C. Adachi, S. R. Forrest, *Phys. Rev. B* **2000**, *62*, 10967.
[46] F.-C. Chen, Y. Yang, M. E. Thompson, J. Kido, *Appl. Phys. Lett.* **2002**, *80*, 2308.
[47] C.-Y. Chuang, P.-I. Shih, C.-H. Chien, F.-I. Wu, C.-F. Shu, *Macromolecules* **2007**, *40*, 247.
[48] J. Liu, Z. Xie, Y. Cheng, Y. Geng, L. Wang, X. Jing, F. Wang, *Adv. Mater.* **2007**, *19*, 531.
[49] J. Luo, X. Li, Q. Hou, J. Peng, W. Yang, Y. Cao, *Adv. Mater.* **2007**, *19*, 1113.
[50] J. Huang, Y. Niu, W. Yang, Y. Mo, M. Yuan, Y. Cao, *Macromolecules* **2002**, *35*, 6080.